Geophysical Research Letters

Increased Extreme Coastal Water Levels Due to the Combined Action of Storm Surges and Wind Waves

Marta Marcos[1,2] (iD), Jérémy Rohmer[3], Michalis Ioannis Vousdoukas[4,5] (iD), Lorenzo Mentaschi[4] (iD), Gonéri Le Cozannet[3] (iD), and Angel Amores[1] (iD)

[1]IMEDEA (CSIC-UIB), Esporles, Spain, [2]Department of Physics, University of the Balearic Islands, Palma, Spain, [3]French Geological Survey (BRGM), Orléans, France, [4]European Commission, Joint European Research Centre (JRC), Ispra, Italy, [5]Department of Marine Sciences, University of the Aegean, Mitilene, Greece

Abstract The dependence between extreme storm surges and wind waves is assessed statistically along the global coasts using the outputs of two numerical models consistently forced with the same atmospheric fields. We show that 55% of the world coastlines face compound storm surge wave extremes. Hence, for a given level of probability, neglecting these dependencies leads to underestimating extreme coastal water levels. Dependencies are dominant in midlatitudes and are likely underestimated in the tropics due to limited representation of tropical cyclones. Furthermore, we show that in half of the areas with dependence, the estimated probability of occurrence of coastal extreme water levels increases significantly when it is accounted for. Translated in terms of return periods, this means that along 30% of global coastlines, extreme water levels expected at most once in a century without considering dependence between storm surges and waves become a 1 in 50-year event.

Plain Language Summary Coastal flooding is caused by a combination of factors, among which storm surges and wind waves are of major relevance due to their potentially large contributions to coastal extreme sea levels and their widespread effects. Based on global scale numerical simulations of these two components, we have investigated the relationship between extreme storm surges and waves along the world coastlines. We find that in more than half of the coastal regions, storm surges tend to be accompanied by large wind waves, thus increasing the potential coastal flooding. Measures for coastal protection often rely on the probability of occurrence of exceedance events (return periods for prescribed water heights), which in turn is determined by the dependence between the contributors to extreme sea levels. The dependency between surges and waves implies that the likelihood of co-occurrence of extremes is higher than assuming these two variables as unrelated. More specifically, the probability of facing a 1 in 100-year event is more than doubled in 30% of the global coastlines when accounting for the dependence between storm surges and waves. Considering these dependencies has a strong impact on return period estimates of extreme high waters and is therefore relevant for the design of coastal defenses.

1. Introduction

Coastal flooding results from the combination of different oceanic and atmospheric drivers, including mean sea level changes, tides, storm surges, waves, river discharge, and rainfall. When two or more of these mechanisms occur simultaneously, flood severity may be exacerbated leading to increased coastal flood risk. Examples of compound flood events include the combination of river discharge and surges (Moftakhari et al., 2017; Ward et al., 2018), rainfall and surges (Wahl et al., 2015, in the U.S. coasts and Wu et al., 2018, in Australia), and rainfall, surge, and waves (Bilskie & Hagen, 2018; Paprotny et al., 2018). If these concurrent events display statistical dependencies (e.g., through a common forcing mechanism), the probability of their joint occurrence (i.e., the chance of two or more extreme conditions occurring at the same time) is higher than that expected considering separately the extremes of each variable, with a consequent increase of the likelihood of coastal flooding.

In areas unaffected by estuarine processes, coastal water levels during extreme events differ from the predicted tides due to (1) the atmospheric storm surge caused by the reduced atmospheric pressure and the effects of winds, (2) the wave setup, an additional contribution to the mean coastal water level (averaged during a few tenths minutes or more; Stockdon et al., 2006), and (3) the wave run-up effects. These phenomena

differ in intensity depending on the offshore storm surge and wave conditions and also due to local coastal settings. Open coasts are obviously the most exposed to the wave effects, with a generally strong wave setup contribution where the submarine offshore slopes are steep (Pedreros et al., 2018; Serafin et al., 2017). However, even in sheltered areas, a significant contribution of the wave setup may be expected (Thompson & Hamon, 1980). Hence, ignoring storm surge, the effects of waves or their compounding effects would intuitively lead to underestimating extreme coastal water levels and their frequencies over a number of coastal localities worldwide that are exposed to the simultaneous action of surges and waves.

Whether relying on observations or reanalysis, extreme coastal water level estimates often presuppose that storm surge events are the only mechanism inducing coastal flooding (Hauer et al., 2016; Hinkel et al., 2014; Muis et al., 2016; Wahl et al., 2017). Indeed, high-frequency coastal tide gauge sea level records are assumed to measure primarily this contribution together with tidal oscillations in many studies relying on observations (Marcos & Woodworth, 2017). However, the same atmospheric disturbances causing storm surges generate also wind waves that may reach the coastlines and affect nearshore water levels. Some previous studies have addressed the problem of joint probability for extremes associated to surges and waves at local or regional scales, as Li et al. (2014) for the Dutch case; Hawkes et al. (2002) Hawkes (2005) for UK, Mazas and Hamm (2017) with an application at Brest (France), Arns et al. (2017) and Ross et al. (2018) in North Sea, and Petrogliakis (2018) along the European coasts. Yet to date, the problem of joint occurrence of storm surges and waves and its impact on coastal flooding has not been addressed globally.

In the present work we perform, for the first time, a global assessment of the dependencies between extreme storm surges and wind waves along the coasts worldwide in a statistical framework. We take advantage of the recent development of accurate, global consistent numerical simulations of storm surges and waves spanning several decades that permit the identification of the coastal regions where extreme storm surges and high waves tend to occur in concurrence as well as the quantification of the dependence of extreme episodes. Due to the modeling setup, we consider only the dependence arising from a common atmospheric forcing, omitting interactions between waves, currents, and sea levels in shallow waters. Our aim is twofold: first, to estimate the changes in the probability of occurrence of compound extreme events along the world coastlines when the storm surges waves dependence is accounted for. Second, to translate these results into return levels of extreme high waters, as these represent one metric of major relevance in the design of coastal protection defenses. Finally, we assess the significance of these dependencies for accurate flood hazard assessment by providing extreme coastal levels for six selected coastal locations situated in different oceanic regions.

2. Data and Methods

2.1. Surge and Wave Hindcasts

The global storm surge and wind wave hindcasts span the period 1979–2014 and are obtained using dynamical models forced by the same atmospheric pressure and wind fields from the European Centre for Medium-Range Weather Forecasts Reanalysis-Interim (ERA-Interim) reanalysis. Storm surges have been generated using the Delft3D-FLOW model with a spatial resolution of 5-km along the coast (10,853 coastal grid points) and temporal outputs every 6 hr. Wind waves have been simulated with the state-of-the-art spectral model WAVEWATCH III (The WAVEWATCH III Development GroupWW3DG, 2016), with varying spatial resolution (saving 4,986 coastal grid points) and 3-hourly temporal resolution. Both data sets have been extensively validated and used as the reference period for present-day storm surge and wave climates (Mentaschi et al., 2017; Vousdoukas et al., 2017, 2018; Vousdoukas, Voukouvalas, Annunziato, et al., 2016). In the present work, each storm surge coastal location has been associated to the closest wave coastal grid point for the combined analyses. Significant wave height (H_s) has been used to build the pairs of storm surge-H_s time series.

2.2. Selection and Dependence of Extreme Surges and Waves

Extreme storm surges and concurrent wind waves have been defined for each pair of surge-H_s time series at every coastal location. To do so, first, independent storm surge episodes exceeding the 99th percentile of each coastal grid point have been selected. Independence among storm surge episodes has been ensured requiring that the events are separated by at least 3 days from each other (following, e.g., Arns et al., 2013; Bardet et al.,
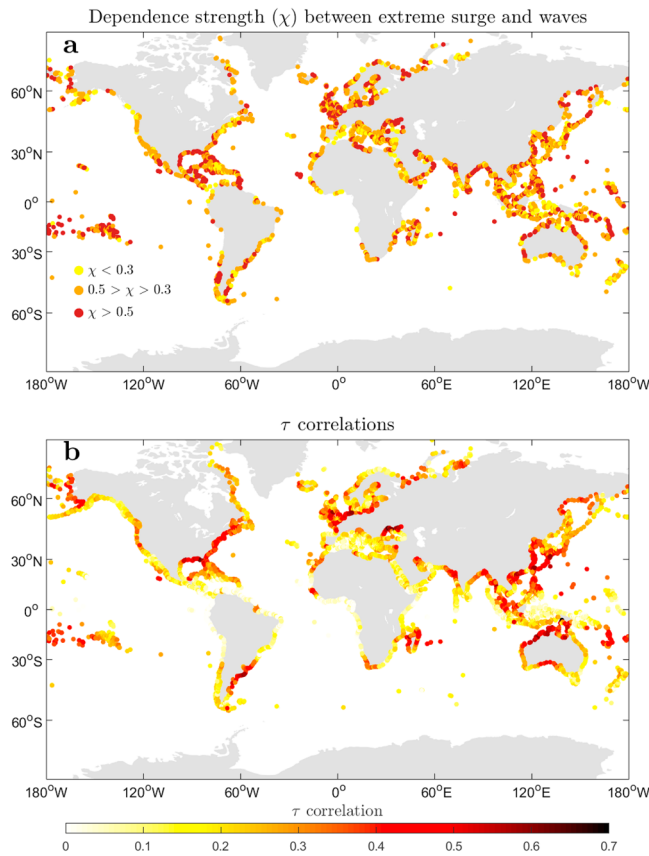
Figure 1. (a) Dependence strength between extreme storm surges (events exceeding the 99th percentile) and concurrent waves, as measured by χ. Blank coastline segments indicate that there is not asymptotic dependence between extremes (limiting value of $\overline{\chi} < 1$, see text for details). (b) Map of Kendall τ correlations between the same extremes storm surges and concurrent waves.

2011; Haigh et al., 2016; Marcos & Woodworth, 2017). Second, for every surge extreme, the highest H_s within an interval of ± 6 hr has been chosen.

Dependence between the extreme storm surge and the corresponding H_s is expected when both values arise from the same forcing event, and it needs to be considered for the computation of joint probability distributions. To measure whether storm surge and wave are dependent when they take large value, we focus on the empirical estimates of the pair $\overline{\chi}$, χ of summary statistics to measure the extremal dependence as defined by Coles et al. (1999). Formally, both indicators are defined as follows:

$$
\chi = \lim_{u \to 1}\left(2 - \frac{\log\left(P(U<u \cap V<u)\right)}{P(U<u)}\right), \overline{\chi}
$$
$$
= \lim_{u \to 1}\left(\frac{2\log\left(P(U>u)\right)}{\log(P(U>u \cap V>u))} - 1\right) \quad (1)
$$

where U and V are the surge and H_s values and u is the quantile level. The first indicator $\overline{\chi}$ is used to screen locations where extremal dependence between both variables is exhibited. This is indicated where the $\overline{\chi}$ tends to 1.0 for very large quantile level u of both variables. In practice, to account for uncertainty in the indicator estimate, we chose to indicate dependency in the case where the confidence interval at 95% for $\overline{\chi}$ excludes the value 1 for all of the largest quantiles. For locations where the value of $\overline{\chi}$ indicates dependency, the second indicator χ (representing the conditional probability of having extreme waves when storm surges are extreme, Coles et al., 1999) provides a measure of the strength of dependence (with values closer to 1 indicating stronger dependence). Figure 1a maps the values of χ for the dependent coastal grid points (those identified as independent according to $\overline{\chi}$ have been blanked). We found dependence in about 55% of the coastlines (6,009 out of 10,853 grid points). Most of the coastal points where storm surge and wave extremes are independent are concentrated in equatorial and tropical regions (blanked in the map), due to the prevalence of remotely generated swells and small surges affecting these coasts and poor representation of cyclonic winds, storm surges,

and waves in global models (see concluding remarks). Likewise, dependence is stronger at midlatitudes, affected by traveling storms that simultaneously generate storm surge and waves. An alternative, measure of the dependence between extremes of two variables is the Kendall rank correlation coefficient τ (see, e.g., Wahl et al., 2015), with higher values of τ indicating stronger dependence. The geographical pattern of extreme dependence shown by τ (Figure 1b) mimics that from χ, with null values in tropical regions, especially along the South American and African coasts, and higher values (up to 0.7) at midlatitudes.

2.3. Modeling Joint Probabilities of Storm Surge and Wave Extremes

As a prior step to the computation of joint probabilities between extreme surge and waves along the coastlines where they are dependent, we require to characterize the univariate storm surge and H_s distributions. We fit a Generalized Pareto distribution (GPD) to excesses of a high threshold value. Here the selection of appropriate thresholds is a key point, as the resulting inferred parameters will be affected by this choice. Standard methods for selecting this threshold rely on visual techniques analysis of quantile-quantile graphs, "mean residual life plots", "modified scale and shape parameters plots" (Coles, 2001), which can hardly be applied in (semi) automatic manner to the roughly 6,000 locations in our data set. To overcome this practical difficulty, we have relied on the recently developed Bayesian cross-validation procedure by Northrop et al. (2017) to select the extreme thresholds for storm surges and H_s at each grid point based on a GPD model. This approach ensures that we minimize the sensitivity of our choice in the final inference of the distribution parameters. In the following, we consider concurrent surge-H_s pairs only when both exceed these selected thresholds. This procedure guarantees the robustness of the univariate distributions, although at the cost of reducing the number of grid points that have enough data to reliably fit a GPD. We have required a
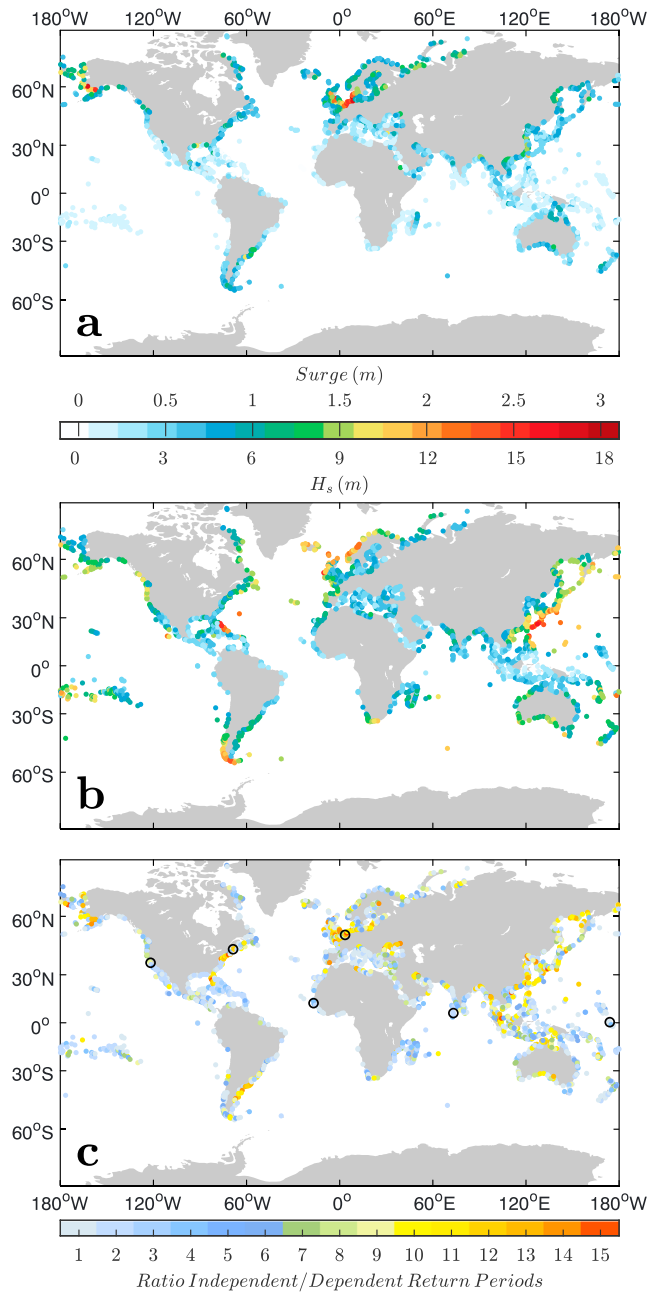
Figure 2. The 50-year joint return levels for surges (a) and for H_s (b) computed for the coastal grid points where there is dependence. (c) Ratio between the joint return period (50-year) and the independent return periods assuming independence, with selected grid points highlighted.

minimum length of 30 data (roughly 1 event per year) to fit the distributions which results in a final set of 5,357 grid points.

We have used copula theory (Coles, 2001; Sklar, 1959) to characterize the dependence between extreme storm surge and H_s. Some recent studies have already successfully applied copulas to reproduce the statistical structure of waves (De Waal & van Gelder, 2005), sea storms (De Michele et al., 2007), and the combination of storm surge and wave extremes (Arns et al., 2017; Sayol & Marcos, 2018). Here we consider five types of copulas of the Archimedean and elliptical families, namely, Clayton, Frank, Gumbel, Gaussian, and t-Student; these have been applied to account for the dependence between univariate GPD distributions at each coastal grid point, through a maximum likelihood procedure. To select the best fitted copula function in each grid point, we minimized the root-mean-square error between the empirical and the theoretical copulas, as in Wahl et al. (2012) and Sayol and Marcos (2018). Other estimators such as Akaike and Bayesian information criteria were also tested, without showing significant differences in the results.

Once the statistical structure of the dependence between extreme storm surges and H_s is characterized, we have computed the joint return levels at each grid point. In the computation of the return levels we have required that both components of sea level extremes exceed their thresholds simultaneously. Following Salvadori and De Michele (2004), this choice is referred therein as the "AND" case, whose probability is expressed as

$$P(U > u \cap V > v) = 1 - F_u(u) - F_v(v) + C[F_u(u), F_v(v)] \tag{2}$$

where U and V are the surge and H_s values, u and v are the corresponding thresholds, C is the copula function related to a prescribed return period, and F refers to the univariate distributions of surges and waves, in this case corresponding to a GPD. The return period RP is related to the joint probability as

$$\text{RP} = \frac{\mu_T}{P(U > u \cap V > v)} \tag{3}$$

with μ_T being the average interarrival time between two successive events. For each grid point this parameter is estimated as the length of the time series (i.e., 36 years) divided by the number of events considered. Note that the same value of $P(U > u \cap V > v)$ may result from different combinations of u and v. Here we have selected the most probable pair of surge-H_s. This approach was also applied in Sayol and Marcos (2018) for a local case study.

If the dependence between storm surges and waves is neglected, the probability of co-occurrence can be computed directly from their univariate distributions. In the "AND" case, when both storm surges and waves are required to exceed their corresponding thresholds, this probability is simply given by

$$P^{\text{indep}}(U > u \cap V > v) = P(U < u) \cdot P(V < v) \tag{4}$$

3. Results

The joint 50-year return levels for storm surges and H_s computed from equation (3) are mapped in Figures 2a and 2b for coastal grid points where there is dependence between both extreme values. As explained above,

these values are not unique but are the most likely given their statistical dependence. The geographical distribution of the return level heights resembles that expected from univariate distributions. For storm surges (Figure 2a), lower values are found in the tropical regions in comparison to midlatitudes. The largest return levels, exceeding 2 m, are located in the North Sea and along the coast of Alaska. In the case of waves (Figure 2b), the lowest values of return levels for H_s are found in the equatorial regions and marginal seas, while higher values (exceeding 12 m) are obtained in more exposed regions in midlatitudes and oceanic islands.

In order to compare the changes in the likelihood of joint occurrence when the dependence structure is accounted for, we have computed the correspondent univariate return periods considering storm surges and H_s as independent. To do so, we first estimated the individual probability of the values of storm surge and H_s mapped in Figures 2a and 2b, using the inferred parameters of their univariate GPD distributions at each grid point. Univariate return levels for a given return period are larger than joint return levels; for example, a point located in 28°N and 82°W, along the Florida coast, has a 50-year joint surge-H_s return level of 61 cm, while the 50-year return level (only surges) is 70 cm. In consequence, these univariate return periods are smaller than 50 years everywhere, as expected. Second, the probability of their joint occurrence was computed as the product of these independent probabilities, following equation (4). Finally, the ratio between this independent return period and the joint (including dependence) 50-year return period is mapped in Figure 2c. These results, therefore, represent the increase factor in the return periods if the dependence between extreme storm surges and waves is neglected. Overall, the median value in the ratio of increase along the coastal regions where there is dependence between surge and waves is 2.5 and maxima values reach a twentyfold increase (Figure 2c).

To be useful for practical purposes, the impact of compound events on return levels must be translated into coastal extreme sea level values, that is, accounting for the impact of surges and waves on water height. The contribution of waves to coastal sea level depends strongly on the topography, bathymetry, bottom types, and even currents at each coastal location, and it ranges from a mean sea level response (known as wave setup) to very high frequency processes (of the order of seconds) such as wave runup. So far, we have only considered the distribution of H_s offshore and given the strong local character of waves transformation when approaching the coast, there is no common methodology that can be applied globally to translate these values into precise coastal sea level contributions. We have therefore opted for estimating the wave contribution to extreme water levels at the coast considering only wave setup, for which we have used the widely applied rule of thumb that quantifies the effect of waves as 20% of H_s in deep waters (e.g., Vousdoukas et al., 2017). Extreme water levels due to storm surges and waves are thus calculated as the addition of storm surge extremes and this wave setup. Six grid points from different ocean regions (indicated with circles in Figure 2 c) have been selected to illustrate the effect of accounting for the dependence in storm surge and wave extremes in return levels of these extreme sea levels (Figure 3). As in Figure 2, joint probabilities (blue lines) are estimated following equation (3), whereas independent probabilities (orange lines) follow equation (4). In four out of five of the cases shown, return periods of extreme coastal water levels are significantly larger if the dependence between storm surges and waves is neglected. For example, in the site located in the North Sea an extreme water level of 3.2 m resulting from the combined action of surges and waves is expected once every 50 years, but its frequency would be estimated in 1 in 532-year event if their dependence was not considered. In contrast, in site located in the Tropical West Pacific the changes in the frequency with and without accounting for dependence are small: the 50-year event of 0.6 m is shifted to a 58-year event.

For completeness we have compared extreme coastal water levels caused by only storm surges, only waves, and both when occurring in concurrence. For the first two cases, we have estimated separately the probabilities of extreme storm surges and waves at each grid point, but this time including in the records all values exceeding the prescribed thresholds and not only those that are concurrent (as in the third case). Note that concurrent cases may not have necessarily selected the highest waves everywhere. Using all data available has increased the number of points that are fitted to the univariate GPDs. The differences obtained between joint surge waves and only storm surges are always positive for the coastal regions analyzed. This implies that the intensity of the compound extreme water levels exceeds everywhere the height of storm surges if these are computed independently for isolated (i.e. not concurrent) events. The median increase in the 50-year return period is 91 cm, with maxima exceeding 3 m in regions with large waves. Likewise, the
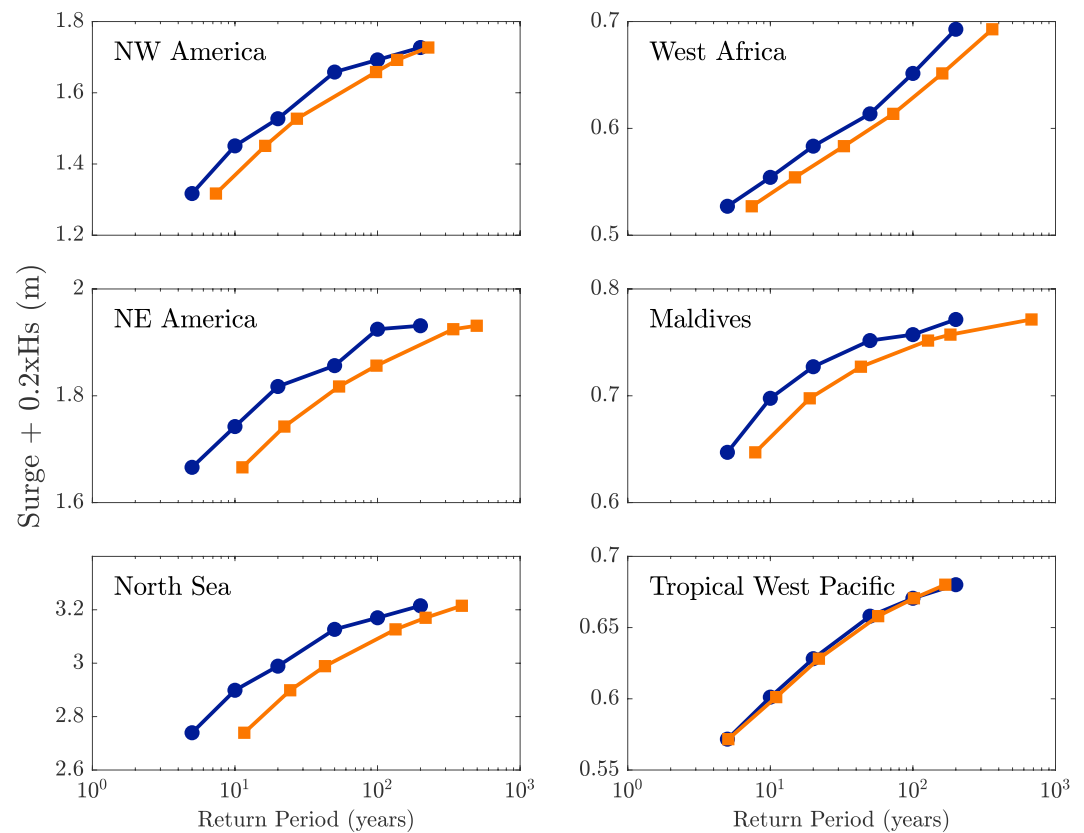
Figure 3. Joint (blue) and independent (orange) return levels of water levels resulting from surge and H_s extremes.

differences between joint storm surge waves and only waves are positive for the 93% of coastal points, with a median increase in the 50-year return level of 53 cm and maximum over 4 m. The points where the effect of only waves is more important and generates higher coastal water level extremes are mostly located in the tropical regions, most likely associated to remote swell waves not linked to local storms.

4. Concluding Remarks

Design of coastal protection strategies must take into consideration all possible forcing mechanisms potentially leading to coastal flooding as well as their interactions. In this respect, earlier numerical efforts have addressed the compound effect of extreme storm surges and wind waves (Dietrich et al., 2012) generally applied to selected case studies of interest, such as hurricane events (Dietrich, Zijlema, et al., 2011; Dietrich, Westerink, et al., 2011). In our approach, we have provided the first global assessment of the effects that the dependence between storm surges and wind waves have in extreme coastal water levels. We have investigated this dependence in a statistical framework. The co-occurrence of these two major drivers of extreme coastal sea level has been identified in 55% of the global coastlines, mostly concentrated at middle to high latitudes. Along the majority of these coastal regions with dependence, the joint surge wave effects exceed that of the individual forcings, with only a few exceptions in tropical locations that are affected by remotely generated strong swell waves. Hence, it is important to consider both mechanisms together with their dependence.

The dependence between extreme storm surges and waves, explained by a common atmospheric origin, increases the likelihood of their joint occurrence in comparison to that of statistically independent events. This is translated into higher coastal flood risks. For example, in terms of return periods, the 50-year return period of joint storm surges and waves is at least doubled, if their dependence is neglected, in roughly 30% of the global coastlines (~50% of those coastal regions where dependence has been identified). In other words, in these locations, an event expected at most once in 100 years without considering dependences between

surges and waves, is revealed in, at least, 1 in 50-year event once they are accounted for. Likewise, a fivefold (tenfold) increase in the 50-year return period is found in nearly 20% (8%) of the global coastlines. Therefore, the estimation of return periods, which is an essential metric for the calculation of coastal allowances and design of defenses (Hunter, 2012), may be significantly biased low if the storm surges and waves hitting the coasts are presumed to occur independently from each other.

Our results are based on the outputs of two storm surge and wave global hindcasts that have been forced consistently with the same atmospheric fields (Mentaschi et al., 2017; Vousdoukas, Voukouvalas, Annunziato, et al., 2016). Numerical models provide the continuous spatiotemporal coverage that is necessary to perform a global assessment, but they also have limitations. In particular, comparisons with in situ data have demonstrated that hydrodynamic models perform satisfactorily at midlatitudes where extreme sea levels are mostly caused by extratropical atmospheric perturbations (Muis et al., 2016; Vousdoukas, Voukouvalas, Mentaschi, et al., 2016), but these global scale models often fail to capture the extreme storm surges associated to tropical cyclones (Muis et al., 2016: Bloemendaal et al., 2018) and so do the wind wave models (Vousdoukas et al., 2018). In consequence, our findings likely underestimate the dependence and the intensity of surge and wave extremes in areas prone to tropical cyclones, due to the numerical runs that we have used. In these areas, regional studies have demonstrated better capabilities to jointly model storm surges and waves generated by tropical cyclones (e.g., Hu & Muller-Karger, 2007; Hope et al., 2013; Bilskie et al., 2016, all in the Gulf of Mexico). On the other hand, the hindcasts used here have a time span of 36 years, which is insufficient to explore the nonstationary behavior of extreme events that has been observed in both storm surges (e.g., Marcos & Woodworth, 2017) and waves (e.g., Méndez et al., 2006). Further research is needed to investigate the impact of this nonstationary character in surge wave dependence, particularly under climate change scenarios for which it has been shown that there is variability in both components (Mentaschi et al., 2017; Vousdoukas, Voukouvalas, Annunziato, et al., 2016).

Finally, it is worth pointing out that we have not considered tides and mean sea level changes in our estimations of return periods. Tides can be a determining factor in coastal flooding, depending on whether the storm effects coincide with a tidal peak. An example is found with the large impacts of storm Xynthia in western France in 2010 when a moderate storm surge coincided with spring high tides (Bertin et al., 2014). Assuming independence between tides and water heights, it is straightforward to incorporate their impact on flood risk assessment (following equation (4)). However, more accurate risk analysis should account for tide-surge interactions, at least in regions where they are nonnegligible (e.g., in the English Channel, Idier et al., 2012, and references therein for other regions). Regarding mean sea level, it has been identified as a major driver of changes in extreme sea levels (Marcos & Woodworth, 2017); thus, the corresponding return periods as those presented here should be adjusted using mean sea level projections for applications in risk assessments (Buchanan et al., 2016; Slangen et al., 2017). Notwithstanding these limitations, our study contributes to improved understanding of global and regional extreme coastal water levels, whose uncertainties are often underestimated and even dominate those of mean sea level rise in many localities for the 21st century (Wahl et al., 2017).

References

Arns, A., Dangendorf, S., Jensen, J., Talke, S., Bender, J., & Pattiaratchi, C. (2017). Sea-level rise induced amplification of coastal protection design heights. *Scientific Reports*, *7*(1), 40171. https://doi.org/10.1038/srep40171

Arns, A., Wahl, T., Haigh, I. D., Jensen, J., & Pattiaratchi, C. (2013). Estimating extreme water level probabilities: A comparison of the direct methods and recommendations for best practice. *Coastal Engineering*, *81*, 51–66. https://doi.org/10.1016/j.coastaleng.2013.07.003

Bardet, L., Duluc, C.-M., Rebour, V., & L'Her, J. (2011). Regional frequency analysis of extreme storm surges along the French coast. *Natural Hazards and Earth System Sciences*, *11*(6), 1627–1639. https://doi.org/10.5194/nhess-11-1627-2011

Bertin, X., Li, K., Roland, A., Zhang, Y. J., Breilh, J. F., & Chaumillon, E. (2014). A modeling-based analysis of the flooding associated with Xynthia, central Bay of Biscay. *Coastal Engineering*, *94*, 80–89. https://doi.org/10.1016/j.coastaleng.2014.08.013

Bilskie, M. V., & Hagen, S. C. (2018). Defining flood zone transitions in low gradient coastal regions. *Geophysical Research Letters*, *45*, 2761–2770. https://doi.org/10.1002/2018GL077524

Bilskie, M. V., Hagen, S. C., Medeiros, S. C., Cox, A. T., Salisbury, M., & Coggin, D. (2016). Data and numerical analysis of astronomic tides, wind-waves, and hurricane storm surge along the northern Gulf of Mexico. *Journal of Geophysical Research: Oceans*, *121*, 3625–3658. https://doi.org/10.1002/2015JC011400

Bloemendaal, N., Muis, S., Haarsma, R. J., Verlaan, M., Apecechea, M. I., de Moel, H., et al. (2018). Global modeling of tropical cyclone storm surges using high-resolution forecasts. *Climate Dynamics*, *52*(7-8), 5031–5044.

Buchanan, M. K., Kopp, R. E., Oppenheimer1, M., & Tebaldi, C. (2016). Allowances for evolving coastal flood risk under uncertain local sea-level rise. *Climatic Change*, *137*(3-4), 347–362. https://doi.org/10.1007/s10584-016-1664-7

Coles, S. (2001). An introduction to statistical modeling of extreme values. In *Springer series in statistics*. London, UK: Springer-Verlag.

Coles, S., Heffernan, J., & Tawn, J. (1999). Dependence measures for extreme value analyses. *Extremes*, *2*(4), 339–365. https://doi.org/10.1023/A:1009963131610

De Michele, C., Salvadori, G., Passoni, G., & Vezzoli, R. (2007). A multivariate model of sea storms using copulas. *Coastal Engineering*, *54*(10), 734–751. https://doi.org/10.1016/j.coastaleng.2007.05.007

De Waal, D. J., & van Gelder, P. H. A. J. M. (2005). Modelling of extreme wave heights and periods through copulas. *Extremes*, *8*(4), 345–356. https://doi.org/10.1007/s10687-006-0006-y

Dietrich, J. C., Tanaka, S., Westerink, J. J., Dawson, C. N., Luettich, R. A., Zijlema, M., et al. (2012). Performance of the unstructured-mesh, SWAN1ADCIRC model in computing hurricane waves and surge. *Journal of Scientific Computing*, *52*(2), 468–497. https://doi.org/10.1007/s10915-011-9555-6

Dietrich, J. C., Westerink, J. J., Kennedy, A. B., Smith, J. M., Jensen, R. E., Zijlema, M., et al. (2011). Hurricane Gustav (2008) waves and storm surge: Hindcast, synoptic analysis, and validation in southern Louisiana. *Monthly Weather Review*, *139*(8), 2488–2522. https://doi.org/10.1175/2011MWR3611.1

Dietrich, J. C., Zijlema, M., Westerink, J. J., Holthuijsen, L. H., Dawson, C. N., Luettich, R. A., et al. (2011). Modeling hurricane waves and storm surge using integrally-coupled, scalable computations. *Coastal Engineering*, *58*(1), 45–65. https://doi.org/10.1016/j.coastaleng.2010.08.001

Haigh, I. D., Wadey, M. P., Wahl, T., Ozsoy, O., Nicholls, R. J., Brown, J. M., et al. (2016). Spatial footprint and temporal clustering of extreme sea level and storm surge evens around the coastline of the UK. *Scientific Data*, *3*, 160107. https://doi.org/10.1038/sdata.2016.107

Hauer, M. E., Evans, J. M., & Mishra, D. R. (2016). Millions projected to be at risk from sea-level rise in the continental United States. *Nature Climate Change*, *6*(7), 691–695. https://doi.org/10.1038/nclimate2961

Hawkes, P. J. (2005). Use of joint probability methods in flood management: A guide to best practice, Defra/Environment Agency and Flood and Coastal Defence R&D Programme.

Hawkes, P. J., Gouldby, B. P., Tawn, J. A., & Owen, M. W. (2002). The joint probability of waves and water levels in coastal engineering design. *Journal of Hydraulic Research*, *40*(3), 241–251. https://doi.org/10.1080/00221680209499940

Hinkel, J., Lincke, D., Vafeidis, A. T., Perrette, M., Nicholls, R. J., Tol, R. S. J., et al. (2014). Coastal flood damage and adaptation costs under 21st century sea-level rise. *Proceedings of the National Academy of Sciences*, *111*(9), 3292–3297. https://doi.org/10.1073/pnas.1222469111

Hope, M. E., Westerink, J. J., Kennedy, A. B., Kerr, P. C., Dietrich, J. C., Dawson, C., et al. (2013). Hindcast and validation of Hurricane Ike (2008) waves, forerunner, and storm surge. *Journal of Geophysical Research: Oceans*, *118*, 4424–4460. https://doi.org/10.1002/jgrc.20314

Hu, C., & Muller-Karger, F. E. (2007). Response of sea surface properties to Hurricane Dennis in the eastern Gulf of Mexico. *Geophysical Research Letters*, *34*, L07606. https://doi.org/10.1029/2006GL028935

Hunter, J. (2012). A simple technique for estimating an allowance for uncertain sea-level rise. *Climate Change*, *113*(2), 239–252. https://doi.org/10.1007/s10584-011-0332-1

Idier, D., Dumas, F., & Muler, H. (2012). Tide-surge interaction in the English Channel. *Natural Hazards and Earth System Sciences*, *12*(12), 3709–3718. https://doi.org/10.5194/nhess-12-3709-2012

Li, F., Van Gelder, P. H. A. J. M., Ranasinghe, R., Callaghan, D. P., & Jongejan, R. B. (2014). Probabilistic modelling of extreme storms along the Dutch coast. *Coastal Engineering*, *86*, 1–13. https://doi.org/10.1016/j.coastaleng.2013.12.009

Marcos, M., & Woodworth, P. L. (2017). Spatiotemporal changes in extreme sea levels along the coasts of the North Atlantic and the Gulf of Mexico. *Journal of Geophysical Research: Oceans*, *122*, 7031–7048. https://doi.org/10.1002/2017JC013065

Mazas, F., & Hamm, L. (2017). An event-based approach for extreme joint probabilities of waves and sea levels. *Coastal Engineering*, *122*, 44–59. https://doi.org/10.1016/j.coastaleng.2017.02.003

Méndez, F. J., Menéndez, M., Luceño, A., & Losada, I. J. (2006). Estimation of the long-term variability of extreme significant wave height using a time-dependent Peak Over Threshold (POT) model. *Journal of Geophysical Research*, *111*, C07024. https://doi.org/10.1029/2005JC003344

Mentaschi, L., Vousdoukas, M. I., Voukouvalas, E., Dosio, A., & Feyen, L. (2017). Global changes of extreme coastal wave energy fluxes triggered by intensified teleconnection patterns. *Geophysical Research Letters*, *44*, 2416–2426. https://doi.org/10.1002/2016GL072488

Moftakhari, H. R., Salvadori, G., AghaKouchak, A., Sanders, B. F., & Matthew, R. A. (2017). Compounding effects of sea level rise and fluvial flooding. *PNAS*, *114*(37), 9785–9790. https://doi.org/10.1073/pnas.1620325114

Muis, S., Verlaan, M., Winsemius, H. C., Aerts, J. C., & Ward, P. J. (2016). A global reanalysis of storm surges and extreme sea levels. *Nature Communications*, *7*, 11969(1). https://www.nature.com/articles/ncomms11969.pdf

Northrop, P. J., Attalides, N., & Philip, J. (2017). Cross-validatory extreme value threshold selection and uncertainty with application to ocean storm severity. *Applied Statistics*, *66*, Part 1, 93–120.

Paprotny, D., Vousdoukas, M. I., Morales-Nápoles, O., Jonkman, S. N., & Feyen, L. (2018). Compound flood potential in Europe. *Hydrology and Earth System Sciences Discussions*, *2018*, 1–34. https://doi.org/10.5194/hess-2018-132

Pedreros, R., Idier, D., Muller, H., Lecacheux, S., Paris, F., Yates-Michelin, M., et al. (2018). Relative contribution of wave setup to the storm surge: Observations and modeling based analysis in open and protected environments (Truc Vert beach and Tubuai island). In J.-S. Shim, I. Chun, & H.-S. Lim (Eds.), *Proceedings from the International Coastal Symposium (ICS) 2018 (Busan, Republic of Korea)*. Journal of Coastal Research, Special Issue No. 85 (pp. 6–10). Coconut Creek, FL: Coastal Education and Research Foundation, Inc.

Petrogliakis, T. I. (2018). Estimations of statistical dependence as joint return period modulator of compound events—Part 1: Storm surge and wave height. *Natural Hazards and Earth System Sciences*, *18*(7), 1937–1955. https://doi.org/10.5194/nhess-18-1937-2018

Ross, E., Sam, S., Randell, D., Feld, G., & Jonathan, P. (2018). Estimating surge in extreme North Sea storms. *Ocean Engineering*, *154*, 430–444. https://doi.org/10.1016/j.oceaneng.2018.01.078

Salvadori, G., & De Michele, C. (2004). Frequency analysis via copulas: Theoretical aspects and applications to hydrological events. *Water Resources Research*, *40*, W12511. https://doi.org/10.1029/2004WR003133

Sayol, J. M., & Marcos, M. (2018). Assessing flood risk under sea level rise and extreme sea levels scenarios. Application to the Ebro Delta (Spain). *Journal of Geophysical Research: Oceans*, *123*, 794–811. https://doi.org/10.1002/2017JC013355

Serafin, K. A., Ruggiero, P., & Stockdon, H. F. (2017). The relative contribution of waves, tides, and non-tidal residuals to extreme total water levels on US West Coast sandy beaches. *Geophysical Research Letters*, *44*, 1839–1847. https://doi.org/10.1002/2016GL071020

Sklar, A. (1959). *Fonctions de repartition a n dimensions et leurs marges* (pp. 229–231). Paris, France: Publications de l'Institut de Statistique de l'Universit e de Paris.

Slangen, A. B. A., van de Wal, R. S. W., Reerink, T. J., de Winter, R. C., Hunter, J. R., Woodworth, P. L., & Edwards, T. (2017). The impact of uncertainties in ice sheet dynamics on sea-level allowances at tide gauge locations. *Journal of Marine Science and Engineering*, *5*(2), 21. https://doi.org/10.3390/jmse5020021

Stockdon, H. F., Holman, R. A., Howd, P. A., & Sallenger, A. H. (2006). Empirical parameterization of setup, swash, and runup. *Coastal Engineering*, *53*(7), 573–588. https://doi.org/10.1016/j.coastaleng.2005.12.005

The WAVEWATCH III Development Group (2016) User manual and system documentation of WAVEWATCH III. Tech. Note, MMAB Contrib. (2016)

Thompson, R. O., & Hamon, B. V. (1980). Wave setup of harbor water levels. *Journal of Geophysical Research*, *85*(C2), 1151–1152. https://doi.org/10.1029/JC085iC02p01151

Vousdoukas, M. I., Mentaschi, L., Voukouvalas, E., Verlaan, M., & Feyen, L. (2017). Extreme sea levels on the rise along Europe's coasts. *Earth's Future*, *5*(3), 304–323. https://doi.org/10.1002/2016EF000505

Vousdoukas, M. I., Mentaschi, L., Voukouvalas, E., Verlaan, M., Jevrejeva, S., Jackson, L. P., & Feyen, L. (2018). Global probabilistic projections of extreme sea levels show intensification of coastal flood hazard. *Nature Communications*, *9*(1), 2360. https://doi.org/10.1038/s41467-018-04692-w

Vousdoukas, M. I., Voukouvalas, E., Annunziato, A., Giardino, A., & Feyen, L. (2016). Projections of extreme storm surge levels along Europe. *Climate Dynamics*, *47*(9-10), 3171–3190. https://doi.org/10.1007/s00382-016-3019-5

Vousdoukas, M. I., Voukouvalas, E., Mentaschi, L., Dottori, F., Giardino, A., Bouziotas, D., et al. (2016). Developments in large-scale coastal flood hazard mapping. *Natural Hazards and Earth System Sciences*, *16*(8), 1841–1853. https://doi.org/10.5194/nhess-16-1841-2016

Wahl, T., Haigh, I. D., Nicholls, R. J., Arns, A., Dangendorf, S., Hinkel, J., & Slangen, A. B. A. (2017). Understanding extreme sea levels for broad-scale coastal impact and adaptation analysis. *Nature Communications*, *8*, 16075. https://doi.org/10.1038/ncomms16075

Wahl, T., Jain, S., Bender, J., Meyers, S. D., & Luther, M. E. (2015). Increasing risk of compound flooding from storm surge and rainfall for major US cities. *Nature Climate Change*, *5*(12), 1093–1097. https://doi.org/10.1038/NCLIMATE2736

Wahl, T., Mudersbach, C., & Jensen, J. (2012). Assessing the hydrodynamic boundary conditions for risk analyses in coastal areas: A multivariate statistical approach based on copula functions. *Natural Hazards and Earth System Sciences*, *12*(2), 495–510. https://doi.org/10.5194/nhess-12-495-2012

Ward, P. J., Couasnon, A., Eilander, D., Haigh, I. D., Hendry, A., Muis, S., et al. (2018). Dependence between high sea-level and high river discharge increases flood hazard in global deltas and estuaries. *Environmental Research Letters*, *13*(8), 084012. https://doi.org/10.1088/1748-9326/aad400

Wu, W., McInnes, K., O'Grady, J., Hoeke, R., Leonard, M., & Westra, S. (2018). Mapping dependence between extreme rainfall and storm surge. *Journal of Geophysical Research: Oceans*, *123*, 2461–2474. https://doi.org/10.1002/2017JC013472